The Nature of Proton Shuttling in Protic Ionic Liquid Fuel Cells

*Daniel E. Smith and Darren A. Walsh**

D. E. Smith, Dr. D. A. Walsh
Nottingham Applied Materials and Interfaces Group, School of Chemistry and GSK Carbon Neutral Laboratory for Sustainable Chemistry, The University of Nottingham, Nottingham NG7 2TU, UK

E-mail: darren.walsh@nottingham.ac.uk

Keywords: fuel cell, ionic liquid, oxygen-reduction reaction, electrocatalysis

It has been proposed that protic ionic liquids (PILs) such as diethylmethylammonium triflate could be used as the electrolytes in nonhumidified, intermediate-temperature H_2 fuel cells, potentially offering the prospect of high conductivity and performance, even under anhydrous conditions. In this contribution, we use a combination of electroanalytical chemistry and fuel-cell polarization analyses to demonstrate for the first time that the pure PILs cannot support proton shuttling between the electrodes of fuel cells. Only through the inclusion of dissolved acidic or basic proton shuttles can viable protic ionic fuel cells be fabricated, which has major consequences for the use of these neoteric electrolytes in fuel cells.

While low-temperature proton-exchange membrane fuel cells are promising for vehicular transport, the cost, performance and stability of the required Pt-based electrocatalysts are major commercial stumbling blocks.[1] Moreover, the low operating temperature of these devices makes heat removal and water management in the devices significant challenges. The development of 'intermediate-temperature' fuel cells that operate in the range 100-300 °C offers several potential advantages over low-temperature cells, including the use of non-precious-metal electrocatalysts, simplification of heat and water management, and improved tolerance to fuel contaminants such as CO and SO_2.[2] The most common class of electrolyte membranes for fuel cells operating at >100 °C are H_3PO_4-doped polybenzimidazole (PBI) membranes, with proton conductivities of about 0.1 S cm^{-1}.[3] However, leaching of H_3PO_4

from the membranes causes a drastic drop in membrane proton conductivity, and degradation of the polymer membranes can occur due to the attack by reactive-oxygen species such as H_2O_2, •OH, and •OOH.[4]

The limitations of electrolytes such as H_3PO_4-doped PBI has led to the use of protic ionic liquids (PILs) as electrolytes for intermediate-temperature fuel cells, which was pioneered most notably by Watanabe and co-workers.[5] PILs can be formed by transferring protons from a range of Brønsted acids to Brønsted bases, and exhibit very low vapor pressures and inherent conductivity.[6] The most promising PIL for use in fuel cells is diethylmethylammonium triflate, [dema][TfO] (**Scheme 1**), which is thermally stable to 360 °C (Figure S1), electrochemically stable over an almost 4-V wide potential window (Figure S2), and exhibits an anhydrous conductivity of 68 mS cm^{-1} at 150 °C.[5a] It has been proposed that PILs can shuttle H^+ ions between the electrodes of fuel cells *via* the cations of the PIL; protonation of the parent base diethylmethylamine (which is denoted dema) upon anodic oxidation of H_2 yields protonated $[dema]^+$ cations (Equation 1), which are subsequently deprotonated at the cathode (Equation 2):[7]

$$H_2 + 2dema \rightarrow 2[dema]^+ + 2e^- \quad (1)$$

$$½O_2 + 2e^- + 2[dema]^+ \rightarrow 2dema + H_2O \quad (2)$$

resulting in the net reaction between H_2 and O_2:

$$H_2 + ½O_2 \rightarrow H_2O \quad (3)$$

In this communication, we demonstrate that this H^+-ion shuttling mechanism cannot occur effectively in cells containing the pure PIL, and that fuel cells require the use of "non-stoichiometric" PILs containing added acids or bases. These observations have significant consequences for the development of protic ionic liquid-based fuel cells; addition of corrosive acids or volatile bases to PIL electrolytes could counter some of the reasons for using an ionic liquid-based electrolyte in the first place and we discuss these implications.

The dashed, red, and blue lines in Figure 1A show cyclic voltammograms (CVs) of [dema][TfO], O_2-saturated [dema][TfO], and O_2-saturated [dema][TfO] containing 0.1 mol dm^{-3} of the parent triflic acid (TfOH), respectively. The reference electrode in each case was a Pd/H reference electrode (see Experimental Section for details).[8] Comparison of the dashed and red lines shows that the oxygen-reduction reaction (ORR) results in a large cathodic wave with an onset potential of about 0.4 V. The limiting current density, j_L, is about 3.5 A cm^{-2} and corresponds to the formation of H_2O (see Reference 9). In the acidified PIL, the entire ORR wave appears at a more positive potential, and has an onset potential of about 1.1 V. j_L in the pure and acidified PILs are similar, indicating that the ORR in the acidified PIL also yields H_2O. The positive shift of the ORR potential upon acidification of the PIL can be explained by considering the proton donor taking part in the ORR in each case. In pure [dema][TfO], the only protons available to take part in the reaction are those on the PIL cations (pK_a 10.6[10]), yielding dema (Equation 2), whereas the ORR at positive potentials in the acidified PIL involves protons from the added TfOH (pK_a −14[10]):

$$\tfrac{1}{2}O_2 + 2e^- + 2TfOH \rightarrow 2[TfO]^- + H_2O \qquad (4)$$

To explore whether the ORR potential depends generally on the pK_a of the added protic species, voltammograms of samples of O_2-saturated [dema][TfO] containing various acids were recorded (Figure 1B). While a clear j_L cannot be identified in all cases, j_L generally reaches

approximately 3.5 mA cm^{-2} in the presence of each acid, indicating that the product is H_2O in each case. The ORR half-wave potential, $E_{1/2}$, shifts positive by about 50 mV per aqueous pK_a unit in the range $-3 < pK_a < 10$ (Figure 1C), which is close to that expected for the ORR involving a generalized proton donor and to that observed previously using an aprotic ionic liquid.[10] The deviation from linearity at $pK_a < -3$ can be attributed to solvent levelling, wherein the supporting PIL acts as a buffer.[10]

To estimate the impact of protic additives on operation of [dema][TfO]-based H_2 fuel cells, the relative potentials of the hydrogen-oxidation reaction (HOR) and the ORR were examined using cyclic voltammetry. Figure 2A shows voltammograms of H_2-saturated [dema][TfO] and O_2-saturated [dema][TfO] containing 0.1 mol dm^{-3} TfOH. During the positive sweep in the H_2-saturated liquid, anodic current flows positive of about 0.05 V, reaching about 2 mA cm^{-2} and resulting in protonation of the PIL anions (:[8]

$$H_2 + 2[TfO]^- \rightarrow 2TfOH + 2e^- \quad (5)$$

The HOR proceeds according to Equation 5 in both acidified and pure [dema][TfO], as the only site available for occupation by electrogenerated protons are the $[TfO]^-$ anions (Figure S3A). However, the ORR in the acidified PIL involves the added TfOH, which proceeds according to Equation 4. Therefore, the net reaction in a fuel cell containing the acidified PIL should be the reaction between H_2 and O_2 to yield H_2O. In this case, H^+ ions would be shuttled between the anode and cathode of the fuel cell via the TfOH/$[TfO]^-$ couple (Figure 2B). As shown by Figure 2A, the difference between the onset potentials of the ORR and the HOR is close to 0.9 V, corresponding to an open-circuit voltage of 0.9 V in a fuel cell, and as observed for conventional[1b] and PIL-based[5e] H_2 fuel cells.

Figure 2C shows voltammograms of O_2-saturated [dema][TfO] and H_2-saturated [dema][TfO] containing 0.1 mol dm^{-3} dema. dema is a stronger base than $[TfO]^-$ and the HOR

results in protonation of dema (Equation 1) at a significantly lower onset potential (–0.5 V) than in the acidified PIL. The ORR proceeds according to Equation 2 in pure [dema][TfO] and [dema][TfO] containing dema, as the only available protons are those on the $[dema]^+$ cations (Figure S3B). Therefore, the net reaction in a fuel cell containing the PIL with added base would also be oxidation of H_2 to yield H_2O, and the H^+ ions would be shuttled between the anode and cathode via the dema/$[dema]^+$ couple (Figure 2D). As shown by the arrow in Figure 2C, the difference between the onset potentials of the HOR and ORR is also approximately 0.9 V.

Finally, we compared the HOR- and ORR-onset potentials in pure [dema][TfO] using cyclic voltammetry (Figure 2E). As in the case of Figure 2A, the HOR-onset potential is about 0.05 V, corresponding to oxidation of H_2, with concomitant protonation of the $[TfO]^-$ ions (Equation 5). The ORR in this case involves deprotonation of $[dema]^+$ cations, giving the following net reaction:

$$H_2 + ½O_2 + 2[dema][TfO] \rightarrow H_2O + 2dema + 2TfOH \quad (8)$$

That is, the simultaneous HOR and ORR in the PIL could only involve concomitant formation of the parent acid and base from the PIL, a highly endergonic process that offsets the exergonic reaction between H_2 and O_2 (in which $\Delta G^{\ominus} = –237$ kJ mol$^{–1}$[11]). This loss of driving force is illustrated by the almost-overlapping HOR- and ORR-onset potentials in Figure 2E. This analysis was also carried out using the structurally-similar PIL diethylmethylammonium bis[trifluoromethanesulfonyl]imide, and the same behaviour was observed (Figure S4). Therefore, our voltammetric analysis indicates that the PIL electrolyte of the fuel cell should contain either acidic or basic additives to shuttle protons between the electrodes and allow current flow between the anode and cathode. In the absence of a significant concentration of an added proton shuttle, sustainable current should not flow (Figure 2F). The loss of driving force for current flow would prevent the build-up of a significant concentration of the required

proton shuttle (as suggested by Equations 1 and 2). To estimate the concentration of TfOH required to effect fast ORR electrochemistry, we changed the concentration of TfOH in [dema][TfO] and recorded a series of ORR voltammograms. The ORR reaches its mass-transport-controlled rate at a TfOH concentration of 88 mmol dm^{-3} (Figure S5), which is almost two orders of magnitude higher than the saturation concentration of O_2 in [dema][TfO].[12]

To demonstrate that the effects observed during voltammetry of the PILs translate to the operation of fuel cells, we constructed a series of Grove-type fuel cells containing Pt wires immersed in [dema][TfO] and over which H_2 and O_2, respectively, were flowing.[5e] The red line in Figure 3A shows the polarisation curve recorded using a cell containing acidified [dema][TfO] and operating at room temperature. The general shape of the curve is similar to that recorded using conventional fuel cells,[1b] in which the voltage decreases rapidly to about 0.7 V from the open-circuit voltage of about 1.0 V due to kinetic losses within the cell. The voltage then drops approximately linearly as the current density increases due to ohmic losses within the cell and, above 0.5 mA cm^{-2}, the voltage drops significantly due to mass-transport losses within the cell.[13] The blue line in Figure 3A shows a similar polarisation curve recorded using a cell containing 0.1 mol dm^{-3} dema in [dema][TfO]. The open-circuit voltage is similar to that observed using the acidified electrolyte and the general shape of the curve is similar to that recorded when using the acidified electrolyte, demonstrating that proton transport between the anode and cathode is possible. In contrast, when the electrolyte is pure [dema][TfO] (green line in Figure 3A), the cell voltage drops drastically as soon as current starts to flow and decreases to 0.0 V at about 0.1 mA cm^{-2}, demonstrating that the pure PIL could not shuttle protons between the electrodes of the cell effectively, in agreement with the behaviour predicted using analytical voltammetry.

Finally, we consider why others have fabricated functioning cells that contained [dema][TfO] as electrolytes.[5h] We hypothesise that this may be due to the heating that PILs have undergone during synthesis, purification, or operation of PIL-based fuel cells. Heating

PILs can increase the equilibrium concentration of parent acids and bases in PIL, and even loss of the most volatile component yielding a non-stoichiometric PIL,[14] potentially providing the shuttles required transport protons between the anode and cathode of fuel cells. Indeed, a drastic increase in the ORR-onset potential in [dema][TfO] as the PIL temperature was raised from 25 °C to 160 °C was demonstrated previously, indicating that the ORR proceeds via different routes at high and low temperatures.[15] To test this hypothesis further, we heated a sample of [dema][TfO] at 150 °C for 64 hours and then allowed it to cool down to room temperature. Figures 3B and 3C show photographs of the PIL before and after heating. The dark color of the sample that had been heated indicates that some decomposition of the liquid had occurred during heating, a phenomenon that we tentatively attribute to decomposition of dema formed at the elevated temperature. Electroanalysis of the sample that had been heated and then cooled reveals that the ORR potential shifted positive (Figure S6), indicating that a protic contaminant had formed irreversibly in the PIL, changing the mechanism by which O_2 is reduced and effecting the ORR at higher potentials. Therefore, it appears that the formation of non-stoichiometric PILs at elevated temperatures (potentially followed by decomposition and/or loss of the most volatile component) may be responsible for the positive results obtained previously using PIL-based fuel cells. This phenomenon may have been overlooked as the detection of neutral parent species in PILs (or determining the extent of "ionicity" of the liquids) is difficult and usually relies on conductimetric measurements,[16] due to the increase in conductivity caused by addition of neutral species to PILs.[17] As dissolved proton shuttles play such a key role in these devices, we believe they cannot be overlooked any more and that future research in this area should address the optimization of such systems. For example, a potential route to the formation of highly non-stoichiometric PILs that can support proton transport between anodes and cathodes in fuel cells is to use PILs in which the equilibrium composition favors a high concentration of the parent species. The equilibrium composition is related to the difference in the aqueous pK_a of the acids and bases, and it is generally accepted that a "ΔpK_a"

> about 15 results in effectively complete proton transfer from the acids to bases.[18] It will be interesting to investigate whether the use of PILs in which ΔpK_a is significantly less than 15 could provide the species required to transport protons in PIL-based fuel cells. Such cells could potentially even work efficiently at low temperatures. Of course, as ΔpK_a and the ionicity of the PIL decreases, the liquid would become more acidic and its vapour pressure would increase, countering some of the reasons for using PIL electrolytes in the first place and raising concerns of cell corrosion and volatilisation of essential electrolyte components, and potentially limiting cell lifetimes.[19] The deliberate addition of dissolved proton shuttles to highly ionic PILs, while offering a route to effective proton shuttling within such cells, raises similar concerns. We believe that the solution lies in the identification of ionic-liquid compositions that can support relatively high concentrations of dissolved proton shuttles (either added to the liquid or as part of the inherent equilibrium composition of the liquid) and high conductivity, but in which the liquids remain non-corrosive and non-volatile.

In summary, we have described the impact of protic additives on the electrochemical behaviour of PILs for use as electrolytes in intermediate-temperature fuel cells. Electrochemically stable PILs must contain dissolved proton shuttles to effectively shuttle protons between the anode and cathode of PIL-based fuel cells. The use of such compositions raises new challenges that must be addressed, including potential loss of proton-conducting additives by evaporation from the electrolytes and cell corrosion. We believe that the challenge is to identify compositions that can retain the advantages offered by ionic-liquid electrolytes (non-volatility and non-corrosivity), while supporting facile proton transport between the anode and cathode of fuel cells.

Experimental Section

Materials and Apparatus: All chemicals were obtained from Acros Organics, Sigma Aldrich, Merck, VWR Chemicals, or Fischer Scientific, and were used as received. O_2 (99.95%) and H_2 (99.999%), were from BOC gases (Nottingham, UK). Ar (99.999%) was from CryoService (Worcester, UK). Pd wire (0.5 mm diameter, 99.99%) and Pt wire (0.5 mm diameter, 99.997%) was from Alfa Aesar. A modulated speed rotator and Pt and glassy-carbon rotating disk electrodes (RDEs) and rotating ring-disk electrodes (RRDEs) were from Pine Research Instrumentation, Inc (Durham, NC, USA). Electrochemical measurements were performed using a model CHI760C potentiostat from CH Instruments, Austin, TX, USA.

[dema][TfO] was prepared by the dropwise addition of 1 mol dm^{-3} aqueous triflic acid to 1 mol dm^{-3} aqueous *N*,*N*-diethylmethylamine with a 5% molar excess of the base. The reaction mixture was cooled in an ice bath. Excess water was removed by rotary evaporation. The product was then either held under vacuum (5×10^{-2} mbar) at room temperature for 72 h and then at 70 °C for 24 h, or held under vacuum (5×10^{-2} mbar) at 40 °C for 1 week, to remove residual water and base. The liquid was then transferred under vacuum to a glovebox containing a dry N_2 atmosphere (<0.1 ppm O_2 and <0.4 ppm H_2O). Attenuated total reflection Fourier-transform infrared spectroscopy was carried out using a Bruker Alpha Platinum-ATR FTIR spectrometer at 30 °C (Figure S7). The liquid was characterized by ^{1}H, ^{13}C and ^{19}F NMR spectroscopy (Bruker Ascend™ 400 MHz NMR Spectrometer) using a hexadeuterodimethyl sulfoxide solvent (Figures S8-S10). Thermogravimetric analysis (TGA) was carried out using a TA Instruments Discovery instrument under a N_2 atmosphere, and residual water contents were determined using Karl-Fischer titrations (Mitsubishi CA-200 Moisturemeter). Residual water contents were < 100 ppm.

Electrochemical Measurements: The use of Pd/H reference electrodes for electrochemistry in PILs was introduced by Angell.[8] Pd-H electrodes provide stable potentials in PILs, which are defined by the hydrogen-redox equilibrium at the interface between Pd and the PIL. A Pd-H reference electrode was fabricated by sealing a 0.5 mm diameter Pd wire (≈ 2.7 cm long) into

borosilicate glass using a butane flame. Approximately 1.5 cm of the Pd wire was left protruding from the glass sheath to form a Pd rod electrode. A polished Ag contact wire was attached to the Pd wire inside the glass sheath using Ag epoxy (Chemtronics, Kennesaw, GA, USA). The Pd rod was then annealed in a butane flame and immersed in water before H_2 was bubbled over the Pd metal surface for 30 minutes. The rod was then rinsed with deionised water and either dried under a flow of N_2 or Ar, or left covered in air until dry.

A three-electrode electrochemical cell containing a 4.6 mm diameter Pt disk working electrode, a Pt flag counter electrode ($A \approx 0.70$ cm^2) and a Pd/H reference electrode was used for all electrochemical measurements, unless otherwise stated. Prior to use, the Pt electrode was polished using an aqueous suspension of 0.05 μm -alumina (Buehler, Lake Bluff, Illinois) on felt polishing pads, and rinsed thoroughly with deionized water. The Pt flag counter electrode was flame annealed in a butane flame before being rinsed with deionised water. All working and counter electrodes were dried in a glassware oven before use. The cell was charged with 5 mL of [dema][TfO], sealed using rubber septa and bubbled with O_2, H_2 or Ar through a needle for a minimum of 40 minutes, while being stirred by a magnetic stirrer. During voltammetric measurements, a blanket of the appropriate gas was maintained above the PIL. All experiments were carried out at room temperature (22 °C). The effect of heating the PIL on the electrochemical behaviour of the liquid was examined by heating a sample of [dema][TfO] to 150 °C in air for approximately 64 hours using a heating block. After heating, the sample was left to cool to room temperature and was re-saturated with O_2 by bubbling with the gas for 40 min while the liquids was stirred.

To mitigate against any changes in the potential of the Pd/H reference electrode upon addition of acid, base, or gases to the PILs, potentials were adjusted such that the electrochemical window was the same during each analysis. Fuel cell polarisation curves were recorded using a H-cell from Pine Research Instrumentation, Inc (Durham, NC, USA), in which a glass frit separated the two chambers. Each chamber of the cell was filled with 8 mL of

[dema][TfO]. H_2 and O_2 was flowed over the negative and positive electrodes, respectively, and each side of the cell was stirred at 650 rpm during measurements. 0.5 mm-diameter Pt wire electrodes were used as the anode and cathode. The current was increased from ≈ 0.0 A at a rate of 0.25 μA s^{-1} and cell voltage was recorded.

Supporting Information
Supporting Information is available from the Wiley Online Library or from the author.

Acknowledgements
We thank the EPSRC for funding through the Centre for Doctoral Training in Fuel Cells and their Fuels (Project EP/L015749/1) and Project EP/P002382/1. We also thank the University of Nottingham for funding through the Beacon of Excellence in Propulsion Futures.

Received: ((will be filled in by the editorial staff))
Revised: ((will be filled in by the editorial staff))
Published online: ((will be filled in by the editorial staff))

References

[1] a) A. Kongkanand, M. F. Mathias, J. Phys. Chem. Lett. 2016, 7, 1127-1137; b) M. K. Debe, Nature 2012, 486, 43-51.

[2] K. S. Lee, S. Maurya, Y. S. Kim, C. R. Kreller, M. S. Wilson, D. Larsen, S. E. Elangovan, R. Mukundan, Energy Environ. Sci. 2018, 11, 979-987.

[3] J. A. Asensio, E. M. Sanchez, P. Gomez-Romero, Chem. Soc. Rev. 2010, 39, 3210-3239.

[4] Q. F. Li, J. O. Jensen, R. F. Savinell, N. J. Bjerrum, Progr. Polym. Sci. 2009, 34, 449-477.

[5] a) T. Yasuda, H. Kinoshita, M. S. Miran, S. Tsuzuki, M. Watanabe, J. Chem. Eng. Data 2013, 58, 2724-2732; b) M. J. Park, I. Choi, J. Hong, O. Kim, J. Appl. Polym. Sci. 2013, 129, 2363-2376; c) S. Liu, L. Zhou, P. Wang, Z. Shao, B. Yi, J. Mater. Chem. A 2013, 1, 4423-4426; d) H. Nakamoto, M. Watanabe, Chem. Commun. 2007, 2539-2541; e) S.-Y. Lee, A. Ogawa, M. Kanno, H. Nakamoto, T. Yasuda, M. Watanabe, J. Am. Chem. Soc. 2010, 132, 9764-9773;

f) H. Puthen Peediyakkal, J. Yu, H. Munakata, K. Kanamura, Electrochemistry 2019, 87, 35-46; g) J. Thomson, P. Dunn, L. Holmes, J. -P. Belieres, C. A. Angell, D. Gervasio, ECS Trans. 2008, 13, 21-29; h) M. Watanabe, M. L. Thomas, S. Zhang, K. Ueno, T. Yasuda, K. Dokko, Chem. Rev. 2017, 117, 7190-7239; i) D. R. MacFarlane, N. Tachikawa, M. Forsyth, J. M. Pringle, P. C. Howlett, G. D. Elliott, J. H. Davis, Jr., M. Watanabe, P. Simon, C. A. Angell, Energy Environ. Sci. 2014, 7, 232-250.

[6] a) S. Menne, J. Pires, M. Anouti, A. Balducci, Electrochem. Commun. 2013, 31, 39-41; b) T. L. Greaves, C. J. Drummond, Chem. Rev. 2008, 108, 206-237.

[7] M. S. Miran, T. Yasuda, M. A. B. H. Susan, K. Dokko, M. Watanabe, J. Phys. Chem. C 2014, 118, 27631-27639.

[8] J. A. Bautista-Martinez, L. Tang, J. P. Belieres, R. Zeller, C. A. Angell, C. Friesen, J. Phys. Chem. C 2009, 113, 12586-12593.

[9] D. A. Walsh, A. Ejigu, J. Smith, P. Licence, Phys. Chem. Chem. Phys. 2013, 15, 7548-7554.

[10] E. E. Switzer, R. Zeller, Q. Chen, K. Sieradzki, D. A. Buttry, C. Friesen, J. Phys. Chem. C 2013, 117, 8683-8690.

[11] P. Atkins, J. de Paula, J. Keeler, Atkin's Physical Chemistry, 11 ed., Oxford University Press, Oxford, 2018.

[12] S. Mitsushima, Y. Shinohara, K. Matsuzawa, K. Ota, Electrochim. Acta 2010, 55, 6639-6644.

[13] F. Barbir, PEM Fuel Cells Theory and Practice, Elsevier Inc., San Diego, 2013.

[14] a) S. E. Goodwin, D. E. Smith, J. Gibson, R. G. Jones, D. A. Walsh, Langmuir 2017, 33, 8436-8446; b) G. L. Burrell, I. M. Burgar, F. Separovic, N. F. Dunlop, Phys. Chem. Chem. Phys. 2010, 12, 1571-1577.

[15] L. Johnson, A. Ejigu, P. Licence, D. A. Walsh, J. Phys. Chem. C 2012, 116, 18048-18056.

[16] a) J. Stoimenovski, E. I. Izgorodina, D. R. MacFarlane, Phys. Chem. Chem. Phys. 2010, 12, 10341–10347; b) A. Pinkert, K. L. Ang, K. N. Marsh, S. Pang, Phys. Chem. Chem. Phys. 2011, 13, 5136–5143. c) D. Rauber, F. Philippi, J. Zapp, G. Kickelbick, H. Natterab, R. Hempelmann, RSC Adv., 2018, 8, 41639–41650. d) S. Thawarkar, N. D. Khupse, A. Kumar, ChemPhysChem 2016, 17, 1006-1017. e) M. Hoque, M. L. Thomas, M. S. Miran, M. Akiyama, M. Marium, K. Ueno, K. Dokko, M. Watanabe, RSC Adv. 2018, 8, 9790–9794.

[17] a) H. Nakamoto, A. Noda, K. Hayamizu, S. Hayashi, H. Hamaguchi, M. Watanabe, *J.* Phys. Chem. C 2007, *111,* 1541-1548; b) A. Noda, M A. B. H. Susan, K. Kudo, S. Mitsushima, K. Hayamizu, M. Watanabe, J. Phys. Chem. B 2003, *107,* 4024-4033; C. Karlsson, C. Strietzel, H. Huang, M. Sjödin and P. Jannasch, ACS Appl. Energy Mater. 2018, 1, 6451-6462.

[18] M. S. Miran, H. Kinoshita, T. Yasuda, M. A. B. H. Susan, M. Watanabe, Phys. Chem. Chem. Phys. 2012, 14, 5178-5186.

[19] M. S. Miran, M. Hoque, T. Yasuda, S. Tsuzuki, K. Ueno, M. Watanabe, Phys. Chem. Chem. Phys. 2019, 21, 418-426.

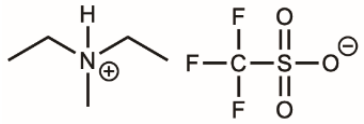

Scheme 1. Structure of diethylmethylammonium triflate.

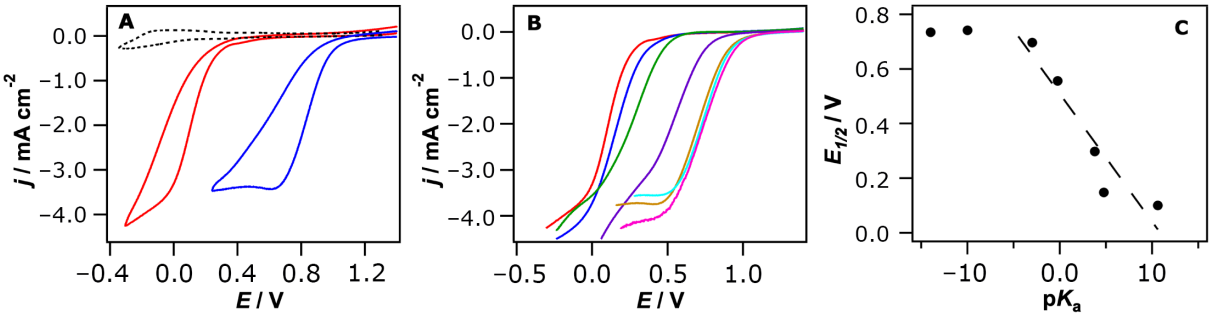

Figure 1. (A) Cyclic voltammograms of O_2-saturated [dema][TfO] (red) and [dema][TfO] containing 0.1 mol dm^{-3} TfOH (blue) recorded using a 5-mm diameter Pt-disk electrode rotating at 1,600 rpm and at a scan rate of 100 mV s^{-1}. The cell temperature was 22 °C. The dashed black line shows the voltammogram of Ar-saturated [dema][TfO]. (B) Linear-sweep voltammograms of O_2-saturated [dema][TfO] containing (from left to right) no added acid, ethanoic acid, formic acid, trifluoroacetic acid, sulfuric acid, perchloric acid, and triflic acid. All voltammograms were recorded using a Pt electrode rotating at 1,600 rpm and at a scan rate of 100 mV s^{-1}. The cell temperature was 22 °C The additive concentration was 0.1 mol dm^{-3} in each case and all potential sweeps began in the negative direction. (C) The ORR half-wave potential versus the aqueous pK_a of (from right to left) [dema][TfO], ethanoic acid, formic acid, trifluoroacetic acid, sulfuric acid, perchloric acid, and triflic acid.

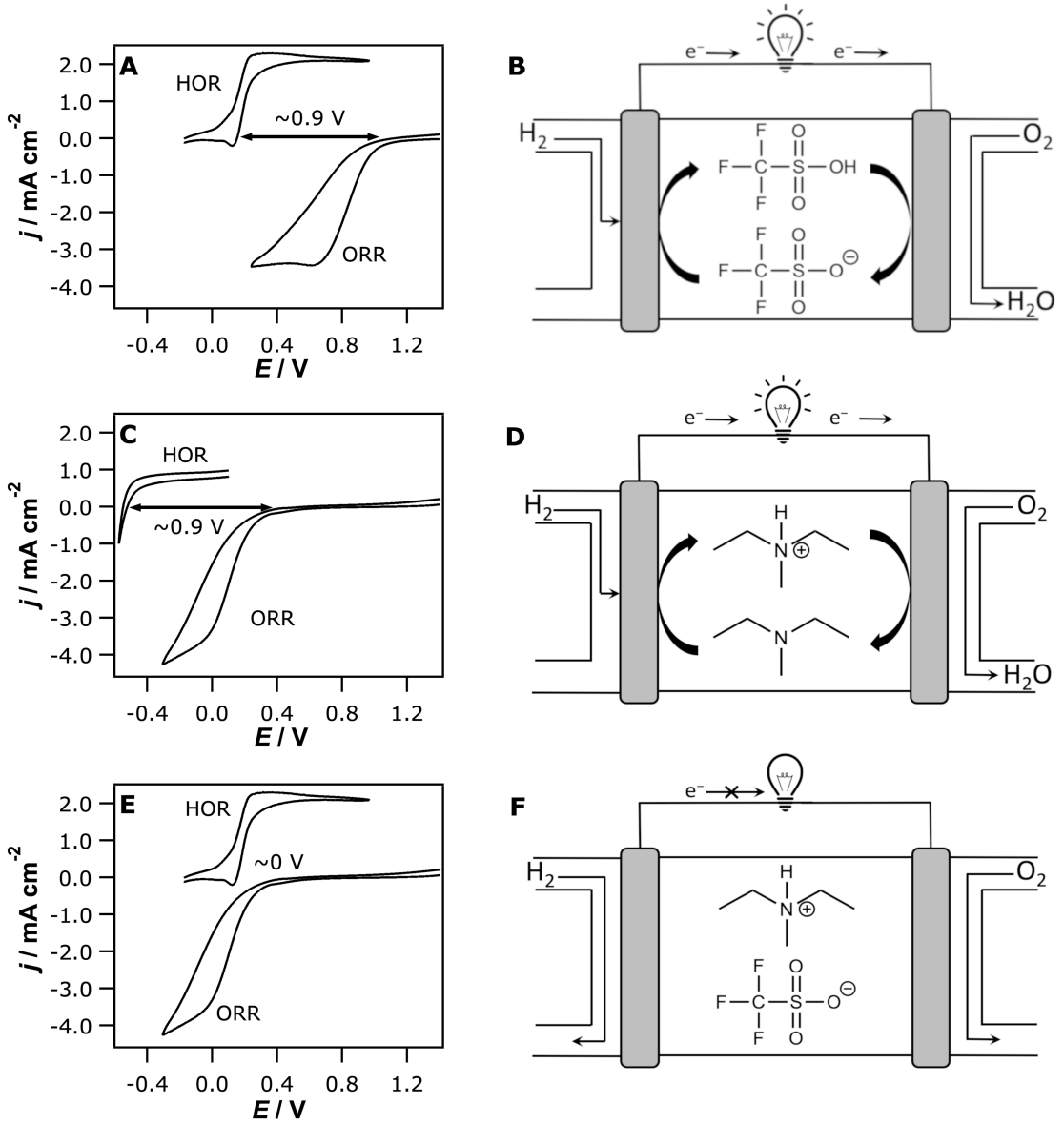

Figure 2. Cyclic voltammograms of (A) H_2-saturated [dema][TfO] and O_2-saturated [dema][TfO] containing 0.1 mol dm^{-3} TfOH, (C) O_2-saturated [dema][TfO] and H_2-saturated [dema][TfO] containing 0.1 mol dm^{-3} dema, and (E) H_2- and O_2-saturated [dema][TfO], respectively. Voltammograms were recorded using a 5-mm diameter Pt electrode rotating at 1,600 rpm and at 100 mV s^{-1}. The cell temperature in each case was 22 °C. The arrow in each frame shows the approximate difference between the ORR and HOR onset potentials. B and D show the proposed operation of [dema][TfO]-based fuel cells containing triflic acid and diethylmethylamine, respectively, as electrolyte additive. F shows that, in the absence of added triflic acid or diethylmethylamine, the cell containing [dema][TfO cannot sustain current flow.

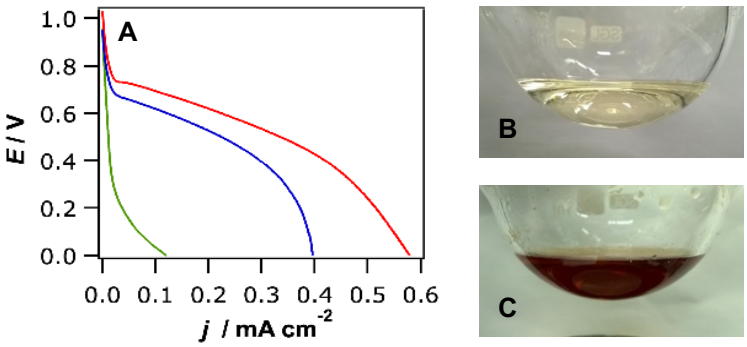

Figure 3. (A) Polarisation curves recorded using a Grove-type fuel cell containing [dema][TfO] (green line), [dema][TfO] containing 0.1 mol dm^{-3} triflic acid (red line), and 0.1 mol dm^{-3} diethylmethylamine (blue line). The current was ramped at 0.25 μA s^{-1} and the cell temperature was 22 °C. H_2 and O_2 were bubbled into the anolyte and catholyte, respectively, at all times and the electrolytes were stirred at 650 rpm. Photographs of [dema][TfO] (B) before and (C) after heating at 150 °C for 64 hours are also shown.

It has been proposed that PILs could be used as the electrolytes in intermediate-temperature H_2 fuel cells. However, pure PILs cannot act as the electrolyte in H_2 fuels cells and only through the addition of protic species can viable fuel cells based on these electrolytes be fabricated.

Fuel cells

D. E. Smith, D. A. Walsh*

The Nature of Proton Shuttling in Protic Ionic Liquid Fuel Cells

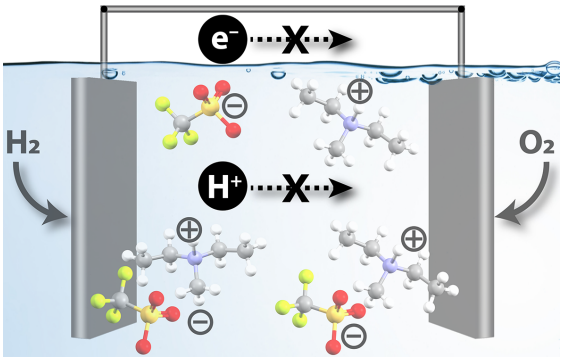

Supporting Information

The Nature of Proton Shuttling in Protic Ionic Liquid Fuel Cells

*Daniel E. Smith, and Darren A. Walsh**

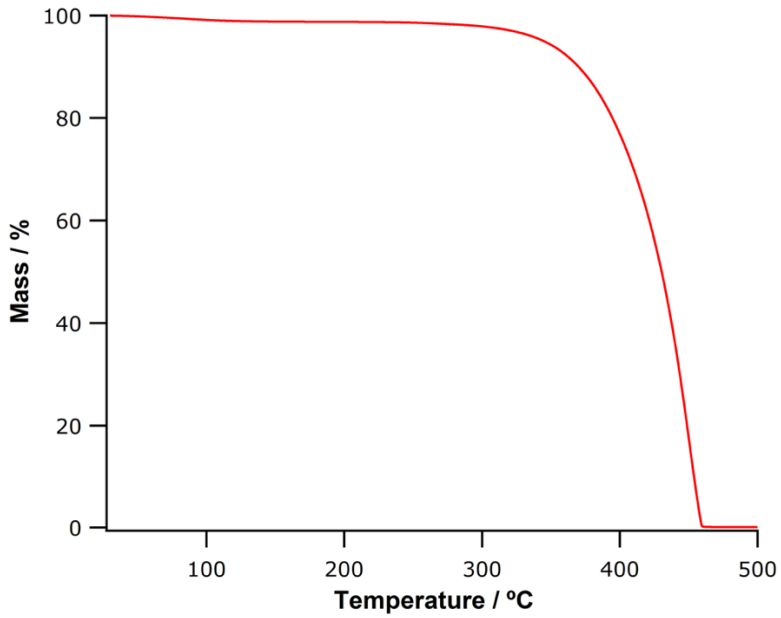

Figure S1. TGA curve of [dema][TfO] under a nitrogen atmosphere.

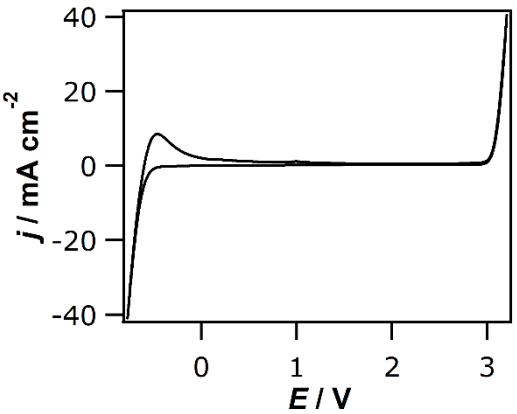

Figure S2. Cyclic voltammogram of [dema][TfO] (≈ 8 ppm H_2O) recorded using a Pt working electrode. The potential cycles begin in a negative-going direction at 100 mV s^{-1}. Below −0.8 V the $[dema]^+$ cation is reduced to H_2 and dema. Electrogenerated H_2 is oxidized in the forward sweep at about −0.5 V. At positive potentials, the $[TfO]^-$ anion is oxidised.

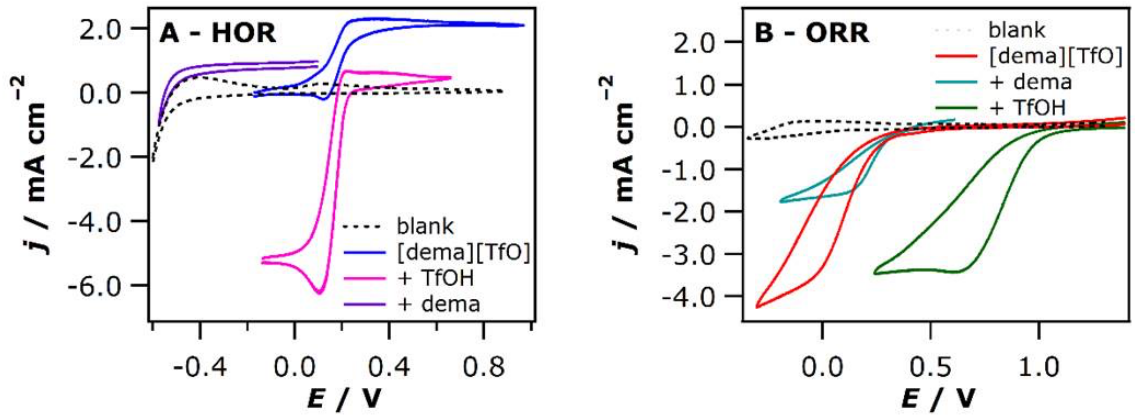

Figure S3. (A) Cyclic voltammograms [dema][TfO] (black dashed line), H_2-saturated [dema][TfO] (blue line), H_2-saturated [dema][TfO] containing 0.1 mol dm^{-3} triflic acid (pink line), and H_2-saturated [dema][TfO] containing 0.1 mol dm^{-3} diethylmethylamine (purple line). H_2 oxidation in the blank and acidified PIL occur at similar potentials and involve protonation of the PIL anions. H_2 oxidation in the presence of diethylmethylamine involves protonation of the base and occurs at significantly less negative potentials. (B) Cyclic voltammograms [dema][TfO] (black dashed line), O_2-saturated [dema][TfO] (red line), O_2-saturated [dema][TfO] containing 0.1 mol dm^{-3} triflic acid (green line), and O_2-saturated [dema][TfO] containing 0.1 mol dm^{-3} diethylmethylamine (light blue line). O_2 reduction in the blank and basified PIL occur at the similar potentials and involve deprotonation of the PIL cations. O_2 reduction in the presence of triflic acid involves deprotonation of the acid and occurs at significantly more positive potentials.

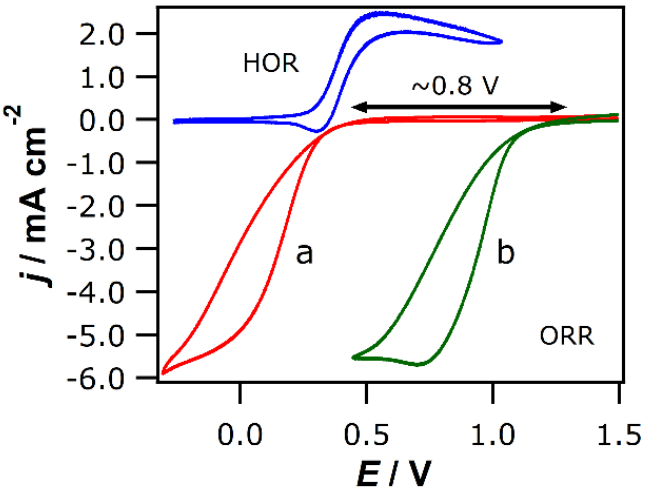

Figure S4. Voltammograms of H_2-saturated [dema][NTf_2] (positive current) and O_2-saturated [dema][NTf_2] in the absence (a) and presence (b) of 0.1 mol dm^{-3} $HNTf_2$ (negative currents). The scan rate is 100 mV s^{-1}. A approximately 0.8 V positive shift in the ORR potential occurred when 0.1 mol dm^{-3} $HNTf_2$ was added to O_2-saturated [dema][NTf_2]. In the absence of added acid, the exergonic oxidation of H_2 in a fuel cell would be offset by the endergonic decomposition of the PIL, meaning that sustained current could not flow.

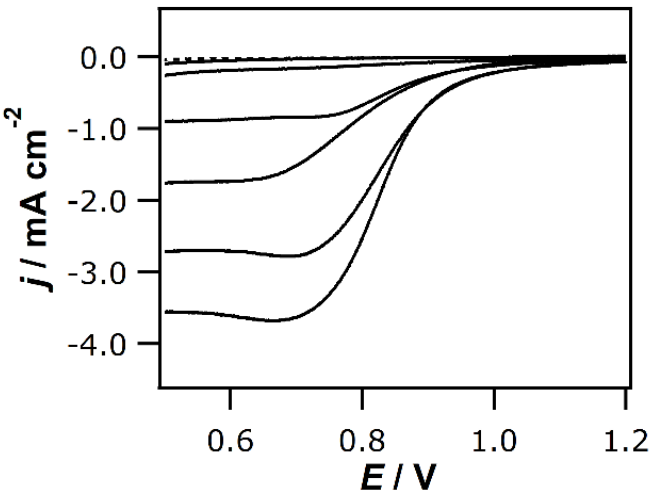

Figure S5. Linear-sweep voltammograms of O_2-saturated [dema][TfO] containing 0, 6, 24, 44, 65, 88 mol dm^{-3} TfOH recorded using a Pt-disk electrode rotating at 1,600 rpm. The dashed black line data shows a voltammograms of Ar-saturated [dema][TfO] recorded at 0 rpm. All voltammograms were recorded at 100 mV s^{-1} and the linear sweeps are in the negative direction. j_L increases as the concentration of TfOH increases, indicating that at low acid concentrations the ORR current is limited by transport of protons, and not O_2, to the electrode surface.

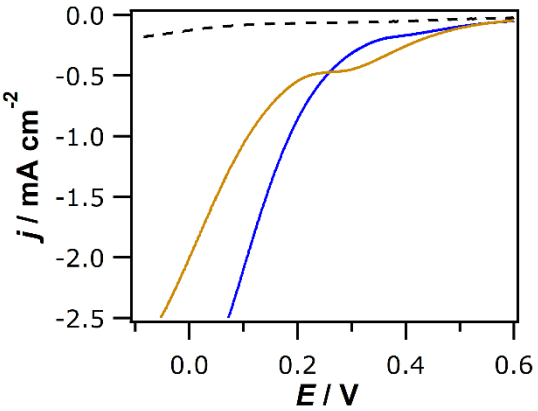

Figure S6. Voltammograms of O_2-saturated [dema][TfO] before and after heating to 150 °C for 64 hours recorded using a Pt-disk electrode rotating at 1,600 rpm. The dashed black line shows the voltammogram of Ar-saturated [dema][TfO] before heating. Each voltammogram was recorded at 100 mV s^{-1} and the sweep was in the negative direction.

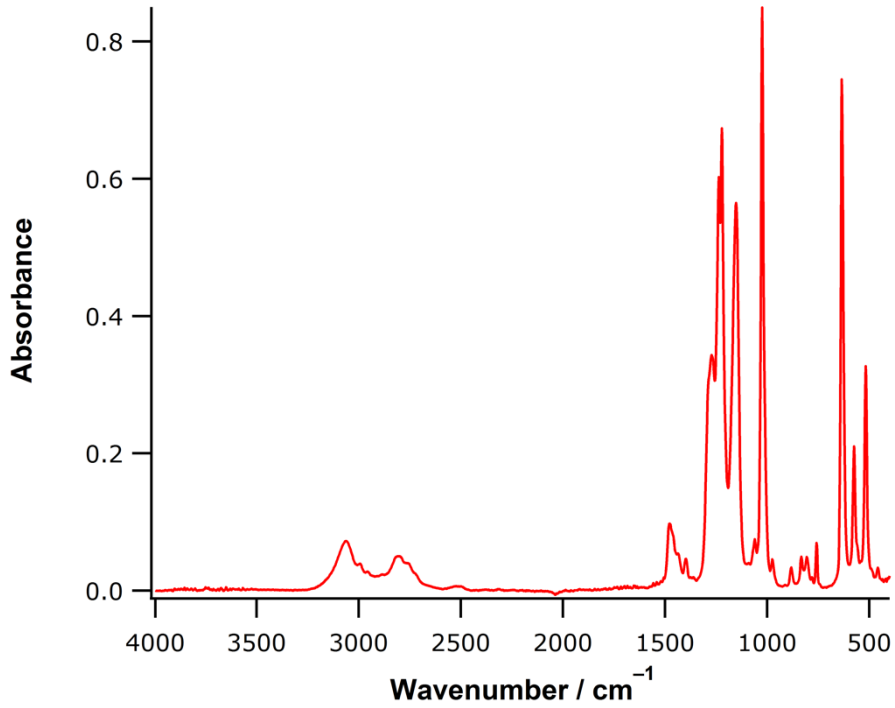

Figure S7. FTIR-ATR absorbance spectrum of [dema][TfO] containing ≈11.7 ppm H_2O recorded at 30 °C

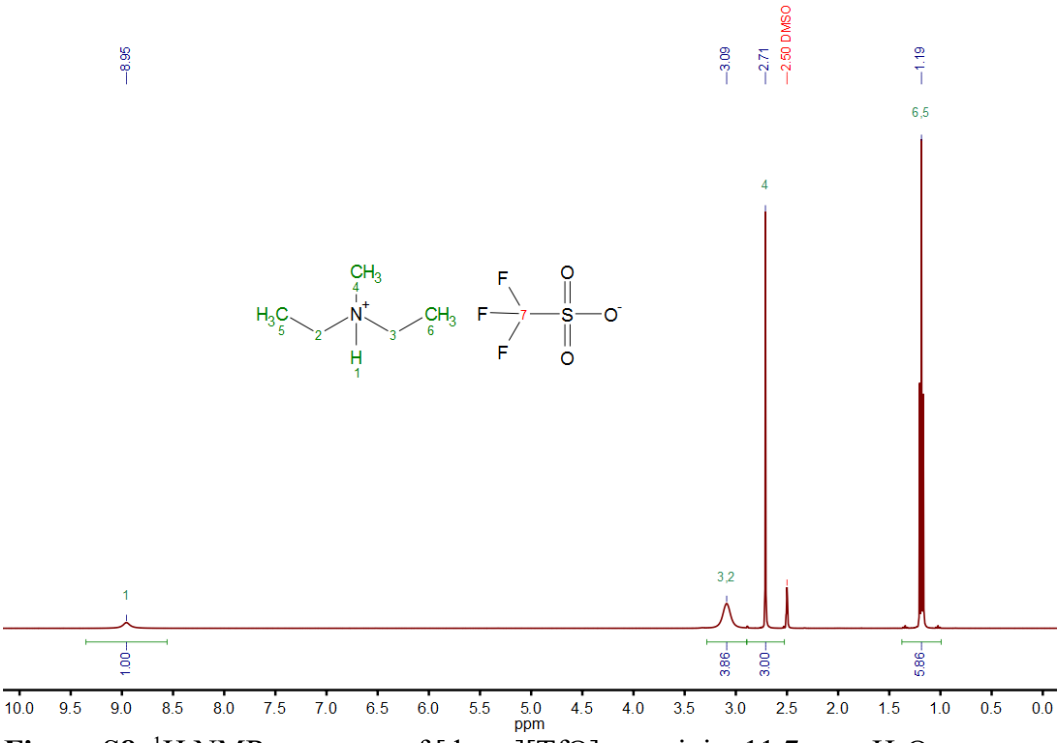

Figure S8. ^{1}H NMR spectrum of [dema][TfO] containing11.7 ppm H_2O.

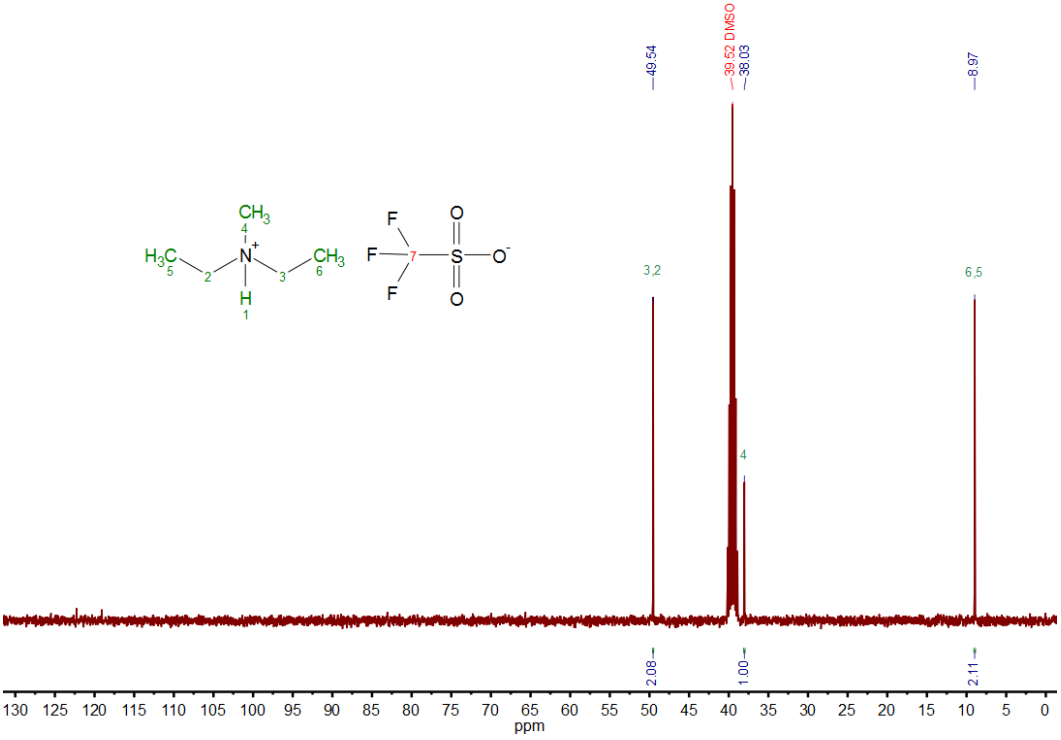

Figure S9. ^{13}C NMR spectrum of [dema][TfO] containing 11.7 ppm H_2O.

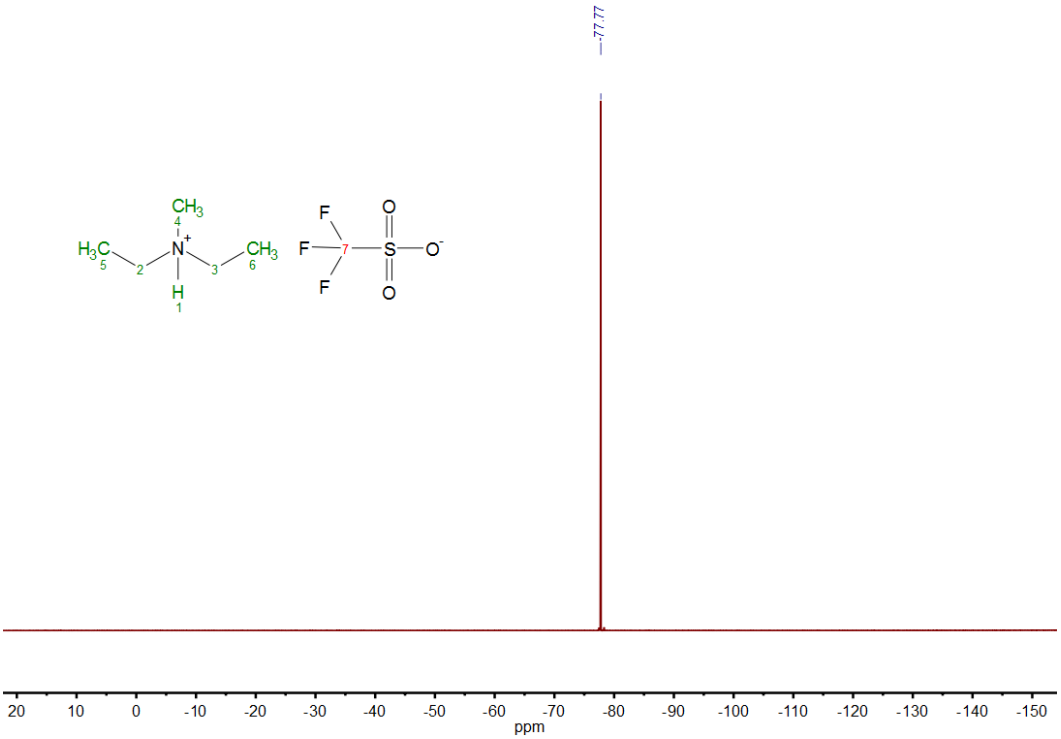

Figure S10. ^{19}F NMR spectrum of [dema][TfO] containing 11.7 ppm H_2O.